Metabolic Brain Disease (2019) 34:593–603
https://doi.org/10.1007/s11011-019-0385-9

ORIGINAL ARTICLE

Astrocyte ablation induced by La-aminoadipate (L-AAA) potentiates remyelination in a cuprizone demyelinating mouse model

Soheila Madadi[1] · Parichehr Pasbakhsh[1] · Fatemeh Tahmasebi[1] · Keywan Mortezaee[2] · Maryam Khanehzad[1] · Fatemeh Beigi Boroujeni[1] · Golaleh Noorzehi[3] · Iraj Ragerdi Kashani[1]

Received: 16 November 2018 / Accepted: 7 January 2019 / Published online: 16 January 2019

Abstract

Chronic demyelination in the central nervous system (CNS) is accompanied by an increase in the number of reactive astrocytes and astrogliosis. There are controversial issues regarding astrocytes and their roles in demyelinating diseases in particular for multiple sclerosis (MS). We aimed to evaluate possible roles for pharmacologic astrocyte ablation strategy using La-aminoadipate (L-AAA) on remyelination in a cuprizone model of demyelination. Male C57BL/6 mice were fed with 0.2% cuprizone for 12 weeks followed by 2-week administration of L-AAA through a cannula inserted 1 mm above the corpus callosum. Rotarod test showed a significant decrease in the range of motor coordination deficits after ablation of astrocytes in mice receiving cuprizone. Results of Luxol fast blue (LFB) and transmission electron microscopy (TEM) for evaluation of myelin content within the corpus callosum revealed a noticeable rise in the percentage of myelinated areas and in the number of myelinated fibers after L-AAA administration in the animals. Astrocyte ablation reduced protein expressions for GFAP (an astrocyte marker) and Iba-1 (a microglial marker), but increased expression of Olig2 (an oligodendrocyte marker) assessed by immunofluorescence. Finally, expression of genes related to recruitment of microglia (astrocyte chemokines *CXCL10* and *CXCL12)* and suppression of oligodendrocyte progenitor cell (OPC) differentiation (astrocyte peptides *ET-1* and *EDNRB*) showed a considerable decrease after administration of L-AAA (for all $p < 0.05$). These results are indicative of improved remyelination after ablation of astrocytes possibly through hampering microgliosis and astrogliosis and a further rise in the number of matured $Olig2^+$ cells.

Keywords Astrocyte ablation · Cuprizone · La-aminoadipate (L-AAA) · Multiple sclerosis (MS) · Remylination · Corpus callosum

Introduction

Multiple sclerosis (MS) is an inflammatory disease of the central nervous system (CNS) (Kieseier and Stüve 2011). MS is characterized by a demyelination process within the grey and white matter, astrogliosis, microgliosis and neuronal damage (Frohman et al. 2006; Karussis et al. 2010; Kieseier and Stüve 2011). MS is divided into acute and chronic phases. In the acute phase, remyelination is partly occurred by migration of oligodendrocyte progenitor cells (OPCs) to the lesion site, while in the chronic phase of the disease there is a progressive demyelination state within the CNS due to lacking migration and differentiation of OPCs to the injured site (Chari et al. 2003; Williams et al. 2007a, b). Following any demyelination events within the CNS, there is a compensatory repairing mechanism for retaining a remyelination process aiming to protect damaged axons from further destructive insults, but it is not so strong to renew the demyelinating events completely (Franklin and Kotter 2008; Skripuletz et al. 2012), so reinforcement of this remyelination process may provide a key therapeutic approach for combating progression of CNS demyelination events (Nessler et al. 2013).

Recent evidence declares that astrocytes play dual and controversial roles in demyelinating diseases (Williams et al.

✉ Iraj Ragerdi Kashani
ragerdi@tums.ac.ir

[1] Department of Anatomy, School of Medicine, Tehran University of Medical Sciences, Poursina Street, Tehran, Iran

[2] Department of Anatomy, School of Medicine, Kurdistan University of Medical Sciences, Sanandaj, Iran

[3] Laboratory Technology Faculty, Khatam Al-Nabieen University, Kabul, Afghanistan

2007a, b). Astrocytes are reported to act in maintaining demyelinated tissues from further damages and attenuating deleterious effects of neuroinflammatory processes on these damaged tissues by release of anti-inflammatory cytokines, such as transforming growth factor (TGF)-β and interleukines (ILs) 10 & 27 (Nair et al. 2008), preventing infiltration of inflammatory cells into the areas of demyelination and creating a permissive milieu for retaining remyelination (Nair et al. 2008; Correale and Farez 2015). There are, however, reports opposing this idea by considering astrocytes as promoters of demyelination through secretion of chemokines that are responsible for recruitment of inflammatory microglial cells toward the lesion sites. This is for restriction of remyelination related processes (Skripuletz et al. 2012; Correale and Farez 2015). These dualities in the functional features for astrocytes would make importance further evaluation of astrocyte ablation strategies for targeting demyelinating injuries.

L-a-aminoadipate (L-AAA) is a glutamate homologue working as an astrotoxin for induction of ablation in astrocytes (Khurgel et al. 1996). Astrocyte ablation induced by L-AAA is a transient process without influencing neuronal density when the cells are under exposure to this agent for about 7 days. L-AAA induces astrocyte ablation through inhibition of glutamate synthesis (Tsai et al. 1996; Gochenauer and Robinson 2001) and uptake (Khurgel et al. 1996; Nishimura et al. 2000) from astrocytes. This ablation further hampers cross talking between astrocytes and microglial cells (Khurgel et al. 1996, Nishimura et al. 2000).

Cuprizone is used as an appropriate agent in induction of demyelination in animal models for evaluation of intrinsic processes of remyelination within the brain. This model has no interference with peripheral immune cells, such as lymphocytes and macrophages (Kipp et al. 2009; Skripuletz et al. 2011). Instead, activation of microglia and astrogliosis are responsible for (fast recovering) acute and (slow recovering) chronic demyelinating lesions in this model (Kipp et al. 2009). The dichotomy of responses from astrocytes to demyelinating insults, as aforementioned, has led us to further investigate a possible contribution of pharmacological astrocyte ablation using L-AAA to remyelinating processes in cuprizone mouse model of chronic demyelination within the CNS.

Materials and methods

Animals and procedures

Seven weeks old male C57BL/6 mice were purchased from Pasteur Institute of Iran, Tehran. The mice were housed under a 12:12-h light–dark cycle in a controlled room temperature (19–22 °C), and they had easy access to Chow and water. All procedures were carried out under the guidance from the ethical committee for Use of Laboratory Animals at Tehran University of Medical Sciences (TUMS).

To induce a chronic demyelination model, mice were fed with 0.2% (*w*/w) cuprizone (biscyclohexanone oxaldihydrazone, Sigma-Aldrich, USA) mixed in standard rodent chow for 12 consecutive weeks. Then animals received L-AAA (Sigma-Aldrich, St. Louis, Missouri) through a cannula inserted 1 mm above the corpus callosum. To explain, at the last week of receiving cuprizone feeding, animals were anesthetized with intraperitoneal injection of a mixture of ketamine (100 mg/kg, K101; Sigma, St. Louis, USA) and xylazine (10 mg/kg, 1644; Serva Feinbiochemica, Heidelberg, Germany) and placed in a stereotaxic apparatus. A 22-gauge guide cannula was implanted at 1 mm above the corpus callosum (stereotaxic coordinates were A/P, −0.5 mm to the bregma; L, +0.5 mm lateral to the midline; and V, 1.7 mm from the skull surface) according to the Paxinos and Franklin atlas (2001). The cannula was fixed to the skull with dental acrylic resin and a stainless steel stylet (30-gauge) was inserted to keep the cannula open before microinjections. The mice were allowed 1 week to recover from surgery and anesthesia, and then they were housed in separate cages after cannula implantation. For intracorpus callosum injection, the stylet was removed from the guide cannula and replaced by 30-gauge injection needle (1 mm below the tip of the guide cannula). L-AAA at dosage 50 μg/1 μL was dissolved in 0.1 M phosphate-buffered solution (PBS, pH 7.4) and injected by a 30-gauge needle to the site of corpus callosum through the cannula at two doses: the first dose was injected at the beginning of week 13, and the second dose was administered at the beginning of week 14 (Khurgel et al. 1996). The needle was remained in the place for 60 s after the injection to facilitate drug diffusion. Mice in the control group received the normal diet, and in the vehicle group were injected with PBS alone. Evaluations were carried out at the end of week 14. There were four groups ($n = 9$): control (Ctrl), cuprizone (CPZ), vehicle (CPZ + PBS) and treatment (CPZ + L-AAA).

Rotarod test

The rotarod test was performed to evaluate motor coordination and balance at the end of week 14 of the experiment. Animals were placed on the rotating drum (Mouse rotarod, UgoBasile, Comerio, Italy) with the rotation set between 4 and 40 rpm for 3 min. The mice were assessed on the rotarod apparatus with three trials per day for three consecutive days, and the interval between the trials was 15 min. One hour before the start of testing, the mice were trained for 3 min. The duration that each mouse was able to maintain its balance on the rotating drum (latency to fall) was recorded.

Tissue preparation

After performing the rotarod test, animals were anesthetized by intraperitoneal injection of ketamine (100 mg/kg) and xylazine (10 mg/kg), and they were undergoing transcardiac perfusion with 0/9% NaCl solution and then fixation with 4% paraformaldehyde (PFA, Merck, Germany) solved in 0.1 M PBS (pH: 7.4) (Ghareghani et al. 2016). The brains were removed, post-fixed in 4% PFA for 24 h and embedded in paraffin. Then, 5 μm coronal paraffin (Merck, Germany) sections were prepared from the collected brains.

Luxol fast blue (LFB) staining

To evaluate demyelination in the corpus callosum, coronal sections were deparaffinized with xylene and rehydrated using decreasing grades of ethanol and stained with LFB (Sigma, USA), as previously described (Acs et al. 2009). Briefly, sections were transferred to the LFB solution at 56 °C overnight, and then they were rinsed in ethanol and distilled water (dH_2O) sweep excess blue stain. Then, color of the staining was differentiated using lithium carbonate solution (Merck, Germany) for 15 s in order to distinguish white matter from gray matter. Slides were transferred to a fresh xylene (Merck, Germany) for two times and mounted with Entellan (Merck, Germany). Images were taken by a light microscope (Olympus, Tokyo, Japan) equipping with a digital camera (Spot camera, Diagnostic Instruments Inc). For evaluation of LFB images, 10 sections per animal were randomly selected with 150 μm intervals at 20x magnification, and the surface area covered with LFB staining was quantified using a densitometric scanning procedure (Image J software, free Java software provided by the National Institute of Health, Bethesda, Maryland, USA). Finally, the percentage of myelinated area in the corpus callosum was calculated by dividing LFB-covered area to the total section area.

Transmission electron microscopy (TEM)

Mice were transcardially perfused with 2% PFA and 2% glutaraldehyde, and corpus callosum was dissected and post-fixed in 2.5% glutaraldehyde for 2 h, washed with 0.1 M PBS and post-fixed in 1% osmium tetroxide. Semi-thin sections (500 nm) were obtained from the samples, and they were stained with 1% toluidine blue to select the targeted areas under observation of light microscopy. Then, ultrathin sections (80 nm) were caught from selected area using a Reichert ultramicrotome and stained with 0.01% uranyl acetate and lead citrate. Finally, sections were observed under TEM electron microscopy (LEO 906 Germany, 100 kV). Photographs of ultrathin cross sections were taken at locations between −0.10 mm and − 0.82 mm bregma, and for each group at least 5 images of the midline corpus callosum region were evaluated at 3000x magnification and the number of myelinated fibers and myelin sheath thickness from 100 myelinated axons were quantified using Image J software.

Immunofluorescence staining

The sections after deparaffinization and rehydration were mixed to a citrate buffer, boiled in a microwave for antigen retrieval and blocked in 10% normal goat serum (Sigma, USA) for 60 min. Then, sections were overnight incubated with primary mouse anti-Olig2 polyclonal (1:1.000; Abcam, UK), anti-Iba-1 polyclonal (1:4000; Wako, Richmond, VA) and anti-GFAP monoclonal (1:1.000; Serotec, Germany) antibodies at 4 °C. Sections were washed in PBS and incubated with anti-mouse IgG secondary antibody (1:500; Sigma, USA) for 2 h at room temperature. Finally, the slides were counterstained with DAPI (Vector labs, UK) and examined under a fluorescence microscope (Olympus IX-71) equipped with a Canon EOS digital camera. Quantification of cells positive for glial cell markers GFAP (for astrocytes), Iba-1 (for microglia) and Olig2 (for oligodendrocytes) within the corpus callosum was manually done using Image J software. The data were collected from three animals per experimental group and four sections with 150 μm intervals for each animal. In each section, five fields with a magnification of 20x were chosen for further interpretation. The cells counted by the software were presented as the cell number per mm^2.

Quantitative real-time PCR (qRT-PCR)

Genes expressions for interferon-inducible protein-10 (CXCL10), interferon-inducible protein-12 (CXCL12), endothelin-1 (ET-1) and endothelin-B receptor (EDNRB) were analyzed in the corpus callosum by qRT-PCR. For analysis of gene expression, animals were culled and the median part of the corpus callosum was collected, and then samples were freezed in liquid nitrogen and stored at −80 °C until preparation of PCR necessary reagents. A QIAGEN RNeasy Kit (Qiagen, Tokyo, Japan) was used for extraction of total RNA, as described previously (Aryanpour et al. 2017). Concentration of the extracted RNA was assessed using a NanoDrop 1000 device (Thermo Fisher Scientific), then reverse RNAs were reverse transcription of the RNA into cDNA was performed using a cDNA synthesis kit (Applied Biosystems, USA). A RealQ Plus 2× Master Mix Green (Ampliqon, Denmark) containing specific primers was analyzed using a StepOne Real-Time PCR system (Applied Biosystems, USA) was used for analysis of gene expression. The expression levels of mRNAs were calculated using a ΔCt-method after normalization of the data collected from the target genes to the mRNA levels of the housekeeping

(reference) β2-microglobulin (β2M) gene. The rate of expression for the target genes was presented as fold change. In the Table 1, the sequences of primers is shown.

Statistical analysis

Statistical analysis was performed using SPSS 22 software, and significant differences between experimental groups were assessed using one-way analysis of variance (ANOVA) followed by Tukey's post-hoc test. Data were presented as mean ± standard error of mean (SEM). *P* value ≤0.05 was considered significant statistically.

Results

Astrocyte ablation decreases motor coordination deficits in cuprizone-induced demyelination

We evaluated the motor coordination and balance of mice by a rotarod apparatus. Latency to fall (from the rotating drum) in the cuprizone group (19 ± 4.932) decreased significantly in comparison to control group (165 ± 5.507) ($p < 0.001$). By contrast, ablation of astrocyte (CPZ + L-AAA group) (67.66 ± 4.91) considerably increased latency to fall from the rotating drum in comparison to the cuprizone group ($p < 0.001$), but it could not retain the time to the level in the control group (Fig. 1). The results indicate that astrocyte ablation is able to improve the cuprizone-induced impairment of motor coordination.

Table 1

Primer name	Primer sequence	Primer length
CXCL10		
Forward:	GCACCATGAACCCAAGTG	18
Revers:	CGTGGCAATGATCTCAACAC	20
CXCL12		
Forward:	GCACTTTCACTCTCGGTCC	19
Revers:	GCGATGTGGCTCTCGAAG	18
ET-1		
Forward:	GGTTTGGACAGACTCAGATC	20
Revers:	TGTCTAACCTGAAAAATGGG	20
EDNRB		
Forward:	ACAGGTGTGAGCTTCTGAG	19
Revers:	AGGACTGCTTCTCCTCCAAG	20
β2M		
Forward:	GGTCTTTCTGGTGCTTGTCTCA	22
Revers:	GTTCGGCTTCCCATTCTCC	19

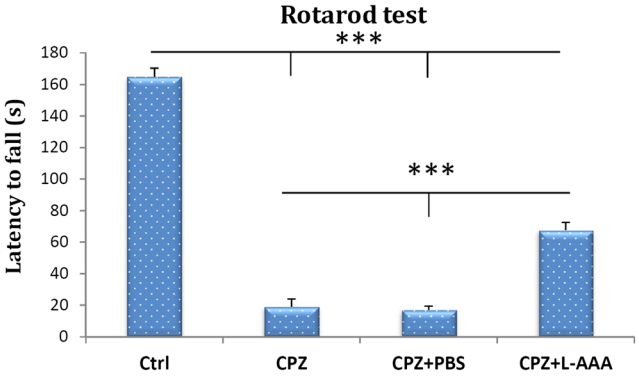

Fig. 1 Monitoring motor coordination and balance by rotarod test in mice receiving cuprizone to evaluate possible effects of astrocyte ablation therapy using L-a-aminoadipate (L-AAA). Mice were assessed for latency to fall from the rotating drum during a period of 180 s. Cuprizone reduced the latency to fall, which was counteracted after administration of L-AAA. ($n = 9$ per group) ***$p < 0.001$ (ANOVA followed by post-hoc analysis)

Effect of astrocyte ablation on remyelination after cuprizone exposure

LFB staining was used to evaluate myelin content within the corpus callosum. As it could be observable for the LFB image sections, there was an apparent reduction in the concentration of blue-stained myelinated areas in animals received cuprizone, whereas after administration of L-AAA, a clear rise in the concentration of myelinated areas was resulted (Fig. 2a–d). Quantitative analysis of myelin content in the body of corpus callosum showed a significant decrease in the percentage of surface area covered by myelin in the cuprizone group (5.33 ± 2.027) compared to the mice fed with normal chow (98 ± 1.154) ($p < 0.001$). On the other hand, L-AAA administration significantly increased the percent of myelination area (59 ± 4.041) compared to the cuprizone group ($p < 0.001$). However, the content of myelin in the astrocyte ablation group was lower than the control group (***$p < 0.001$) (Fig. 2e).

The number of myelinated axons was also evaluated by TEM microscopy that allows observation of the myelin sheath ultrastructure. The images were taken from ultrathin sagittal sections from corpus callosum, and the percentage of myelinated exons and the myelin sheath thickness were analyzed. TME image interpretation revealed an apparent reduction in the number of myelinated axons and the thickness of myelin sheath in the mice receiving cuprizone, while there was a clear rise after receiving L-AAA (Fig. 3a–d). Quantitative data showed that the mean of myelinated fibers was significantly decreased in the cuprizone group (9.67 ± 1.764) in comparison to control (95.33 ± 2.728) ($p < 0.001$), while administration of L-AAA caused a significantly increase in the percentage of myelinated fibers (50.67 ± 3.383 for the CPZ + L-AAA group), as compared to the cuprizone group ($p < 0.001$). This level, however, was less than the percentage of myelinated fibers shown for the control group ($p < 0.001$) (Fig. 3e).

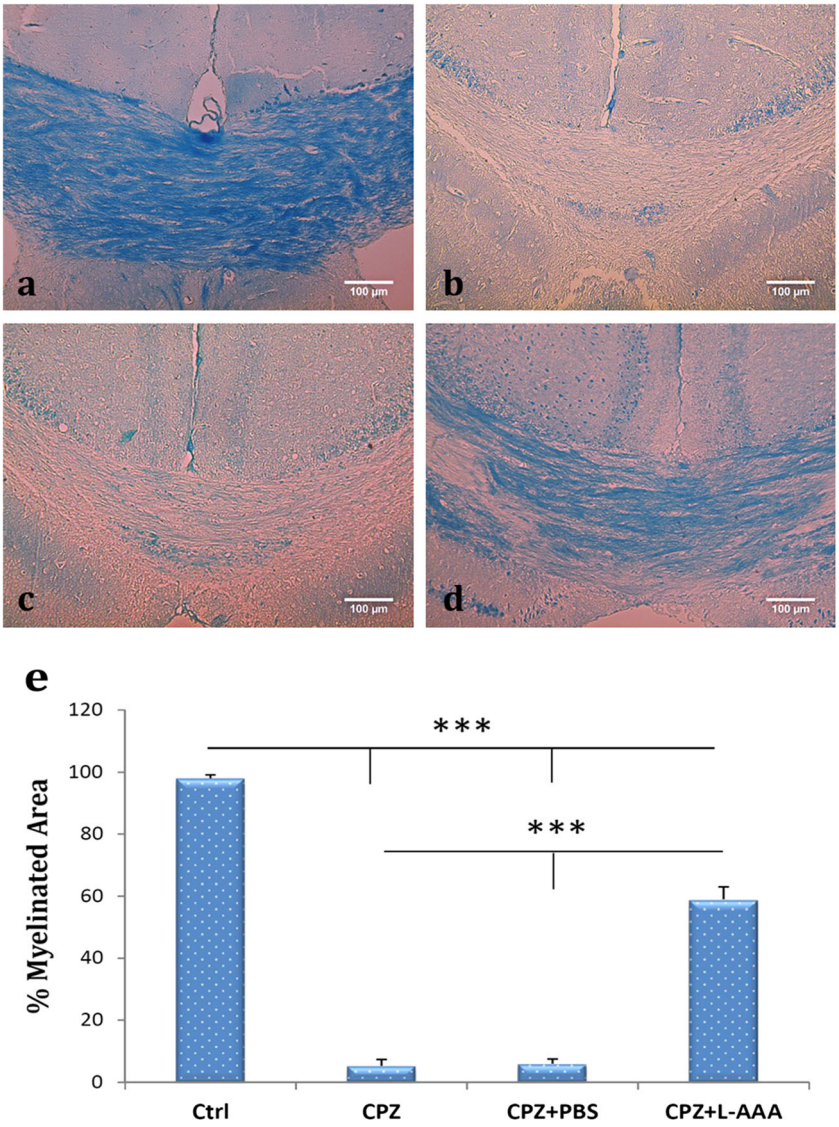

Fig. 2 Luxol fast blue (LFB) staining for evaluation of astrocyte ablation effects (induced by L-a-aminoadipate/L-AAA) on remyelination within the corpus callosum in mice receiving cuprizone. **a** control (Ctrl); **b** cuprizone (CPZ); **c** vehicle (CPZ + PBS); and **d** astrocyte ablation (CPZ + L-AAA). Exposure of mice with cuprizone caused an apparent reduction in the concentration of blue-stained myelinated areas within the corpus callosum, which was abrogated after administration of L-AAA. Quantification of the LFB data showed that the changes in the rate of myelination expressed in percentage were significant among different groups. ($n = 3$ per group) ***$p < 0.001$ (ANOVA followed by post-hoc analysis)

Similarly, the cuprizone group showed a noticeable decrease in the mean myelin sheath thickness (0.051 ± 0.01 μm) compared to the control ($p < 0.001$), whereas treatment with L-AAA increased the thickness of myelin sheath (0.414 ± 0.042 μm for the CPZ + L-AAA group), which was considerable in comparison with the cuprizone group ($p < 0.01$). The rate of thickness of myelin sheath in the L-AAA treated mice was still lower than the rate for the control, and this lower rate was considerable ($p < 0.05$) (Fig. 3f).

Effect of astrocyte ablation on glia

Immunofluorescence staining was performed for assessment of GFAP (an astrocyte marker), Iba-1 (a microglial marker) and Olig2 (an oligodendrocyte marker) presented in the Figs 4, 5 and 6a–d, respectively. As it is understandable from images, astrogliosis (a rise in the level of GFAP) and microgliosis (a rise in the level of Iba-1) and a reduction in the number of oligodendrocyte (a decrease in the level of Oilg2) were evident in the mice exposed to the cuprizone. Administration of L-AAA to induce astrocyte ablation could cause an observable reduction in the rate expressions for GFAP and Iba-1, but it caused an apparent increase in the rate of expression for the Olig2.

Data collected from immunofluorescence were quantified to see whether the changes found from the images were significant statistically. Induction of demyelination by cuprizone caused a robust astrocyte response in the cuprizone (291.66 ± 20.787) group in comparison to control (50.33 ± 4.33) ($p < 0.001$). By contrast, after administration of L-AAA, the number of $GFAP^+$ cells reduced significantly (84.66 ± 5.783) ($p < 0.001$ vs. CPZ group) (Fig. 4e). Similarly, cuprizone addition to the chow significantly increased the number of Iba-1^+ cells in the cuprizone group (152.33 ± 10.333) in comparison to control (16.33 ± 3.527) ($p < 0.001$), whereas L-AAA administration resulted in a significant decrease in the rate of

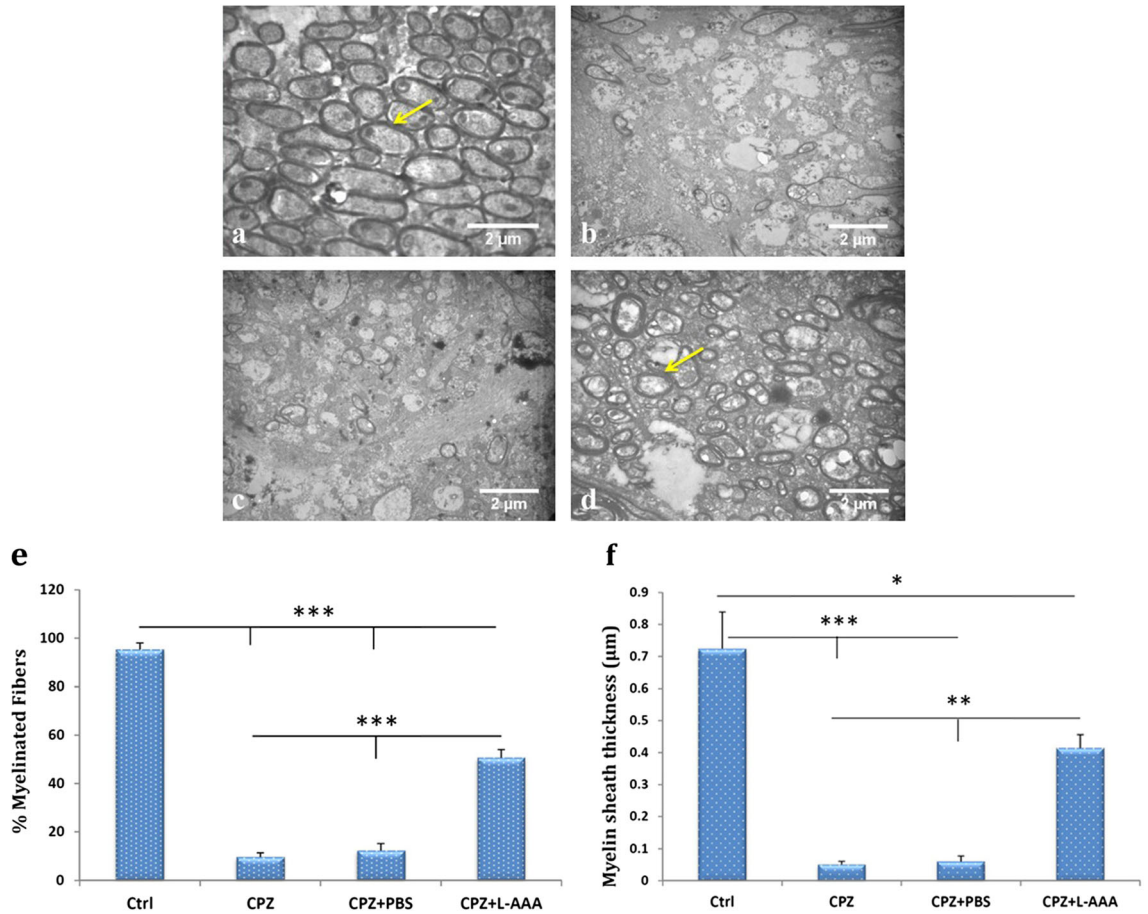

Fig. 3 Transmission electron microscopy (TEM) for evaluation of myelination in the corpus callosum in mice receiving cuprizone for induction of demyelination and further treatment with L-a-aminoadipate (L-AAA). There was an apparent decrease in the number of myelinated fibers and in the thickness of myelin sheath for the cuprizone group, while after administration of L-AAA, the number and the thickness of respective myelin fibers and sheath was increased. **a** control (Ctrl); **b** cuprizone (CPZ); **c** vehicle (CPZ + PBS); and **d** astrocyte ablation (CPZ + L-AAA). Yellow arrows indicate the myelinated fibers. Quantification of TEM data (**e** & **f**) showed that the changes between groups were significant. ($n = 3$ per group) ** $p < 0.01$; and *** $p < 0.001$ (ANOVA followed by post-hoc analysis)

expression for this marker (75 ± 4.932) ($p < 0.01$ vs. cuprizone) (Fig. 5e). Quantification of Olig2 expression showed a considerable fall in the rate of expression for the marker in the cuprizone group (34.33 ± 4.096) ($p < 0.001$ vs. control), while there was a significant rise in the rate of expression for the CPZ + L-AAA group (70.67 ± 10.682) (34.33 ± 4.096) ($p < 0.05$ vs. cuprizone group) (Fig. 6e).

Astrocyte ablation decreased levels of mRNA expression of CXCL10, CXCL12, ET-1 and ENDR-B in the corpus callosum after cuprizone exposure

In this study, we analyzed the levels of mRNA expression of factors contributed to the recruitment of microglia toward demyelinating lesion areas of corpus callosum. CXCL10 and CXCL12 are chemoattractants and inflammatory mediators, and ET-1 and EDNRB are intercellular signaling peptides secreted by astrocytes following demyelinating injury. Animals receiving cuprizone experienced a significant rise in the rate of expressions for all of the chemokines, while after administration of L-AAA, a reversed trend was resulted in which a reduced rate of expressions for the mRNA of the all assessed genes was resulted (for all $p < 0.05$ vs. cuprizone group). Reduction of the chemokines and peptides after administration of L-AAA-induced astrocyte ablation indicates that astrocytes are the major source of these factors in the corpus callosum (Fig. 7).

Discussion

In the present study, we investigated roles for astrocytes in remyelination using chronic cuprizone-induced demyelination followed by administration of L-AAA for induction of astrocyte ablation. We noticed that L-AAA administration could reduce demyelination in mice exposed to the cuprizone. The number of oligodendrocyte ($Olig2^+$ cells) was increased noticeably after astrocyte ablation therapy. This was

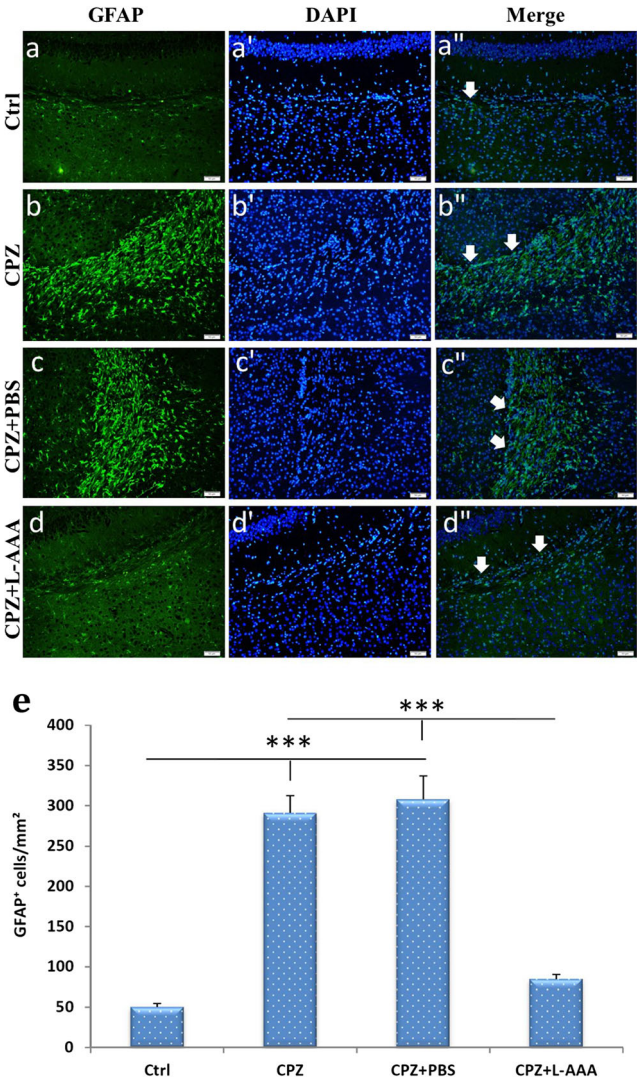

Fig. 4 Immunofluorescence staining for assessment of an astrocyte marker GFAP in the corpus callosum in mice receiving cuprizone for induction of demyelination and further treatment with L-a-aminoadipate (L-AAA). Cuprizone exposure caused an apparent increase in the level of protein expression for GFAP indicative of astrogloisis in the animals. Administration of L-AAA to induce astrocyte ablation could cause an observable reduction in the rate expression for GFAP. Arrows are indicative of GFAP$^+$ cells. Quantification of immunofluorescence data (Graph e) revealed that the alterations in the rate of expression for GFAP in the understudying groups were significant. Scale bars: 50 μm. ($n = 3$ per group) ***$p < 0.001$ (ANOVA followed by post-hoc analysis)

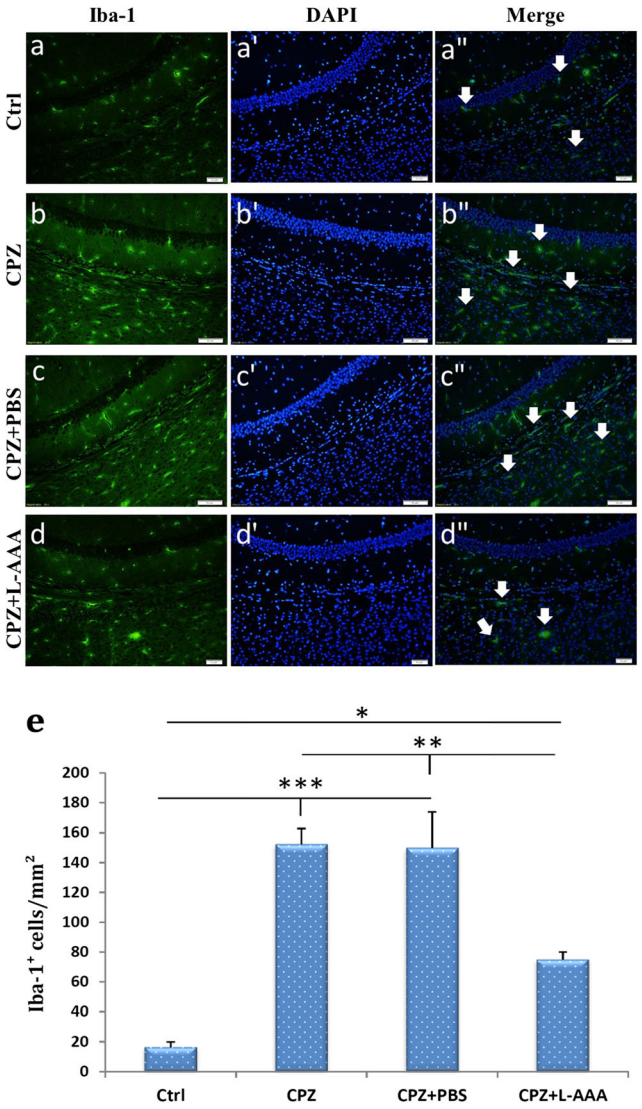

Fig. 5 Immunofluorescence staining for evaluation of a microglial marker Iba-1 in the corpus callosum of mice receiving cuprizone for induction of demyelination and further treatment with L-a-aminoadipate (L-AAA). Cuprizone exposure caused an observable rise in the rate of expression for Iba-1 indicative of microgliosis. Administration of L-AAA to induce astrocyte ablation could cause an observable attenuation in the rate expression for the Iba-1 protein. Arrows are indicative of Iba-1$^+$ cells. Quantification of immunofluorescence data (Graph e) revealed that the alterations in the rate of expression for Iba-1 in the understudying groups were significant. Scale bars: 50 μm. ($n = 3$ per group) * $p < 0.05$, ** $p < 0.01$, and *** $p < 0.001$ (ANOVA followed by post-hoc analysis)

accompanied by a decrease in the number of microglia (Iba1$^+$ positive cells) after such therapy. In agreement with our study, Skripuletz et al. (2012) showed that ablation of astrocytes by ganciclovir in transgenic mice receiving cuprizone could cause a significant decrease in the rate of demyelination within the corpus callosum associated with reduction in the number of activated microglia in injury sites. Interestingly, they found a noticeable reduction in the number of Olig2$^+$ cells in astrocyte-ablated transgenic mice, which was in contrary to our results. They reported that myelin debris inhibit OPC differentiation into oligodendrocytes, and ablation of astrocytes reduces the recruitment of microglia as phagocytosing cells to clear damaged myelin sheath (Skripuletz et al. 2012).

There is a compelling evidence for involvement of extracellular matrix (ECM) in regulation of the proliferation and differentiation of OPCs into myelin producing oligodendrocytes, and that any changes in the ECM related signaling in the pathological environment would be preventive for maturation of oligodendrocytes (Baron et al. 2005; Stoffels et al. 2013). Astrocytes have the capacity to

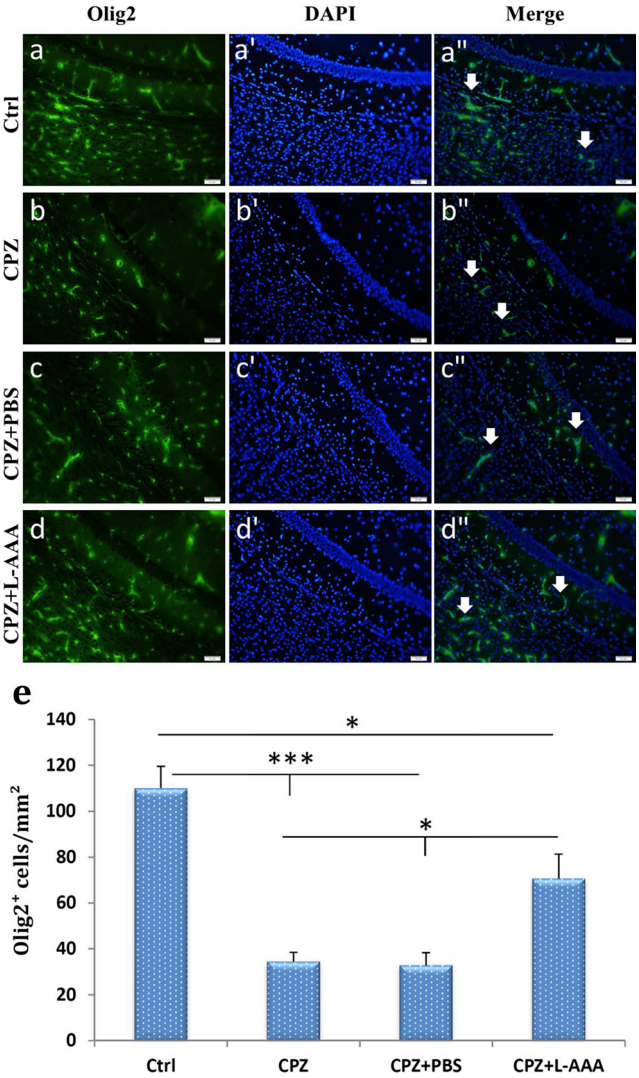

Fig. 6 Immunofluorescence staining for evaluation of an oligodendrocyte marker Olig2 in the corpus callosum of mice receiving cuprizone for induction of demyelination and further treatment with L-a-aminoadipate (L-AAA). Cuprizone exposure caused an observable decrease in the rate of expression for Olig2 indicative of a reduction in the number of myelin-producing oligodendrocyte cells. Induction of astrocyte ablation by administration of L-AAA could cause an observable augmentation in the rate expression for the Olig2 protein. Arrows are indicative of $Olig2^+$ cells. Quantification of immunofluorescence data (Graph e) revealed that the alterations in the rate of expression for Olig2 in the understudying groups were significant. Scale bars: 50 μm. ($n = 3$ per group) * $p < 0.05$ and *** $p < 0.001$ (ANOVA followed by post-hoc analysis)

modify the constituents of ECM in MS by producing a variety of components that directly influence remyelination within the CNS (Clemente et al. 2013). Fibronectin and hyaluronic acid are components of ECM produced by reactive astrocytes in chronic MS lesions that are responsible for stimulation of OPC proliferation but suppression of their further differentiation toward attaining a mature oligodendrocyte phenotype resulting in an impaired remyelination within the CNS (Back et al. 2005; Stoffels et al. 2013, 2015). These are evidences in favor of using astrocyte ablation as a promising strategy in promotion of remyelination-related processes within the CNS lesion areas. However, there are reports suggested that astrocytes could exert dual and even opposing roles in demyelinating diseases by having both protective and destructive functions (Nair et al. 2008; Skripuletz et al. 2012). There are studies suggested that astrocytes could have supportive roles in providing a permissive milieu for maturation and differentiation of OPCs in demyelinating lesions (Nair et al. 2008; Skripuletz et al. 2012; Hammond et al. 2014). A possible claim to support these results possibly is that astrocytes through formation of glial scars are able to act as a physical barrier against infiltration of inflammatory cells into demyelinated areas of CNS (Skripuletz et al. 2012). Voskuhl et al. (2009) reported that ablation of proliferating astrocytes in GFAP–thymidine kinase transgenic mice prevented astrocyte perivascular scar formation which was accompanied with infiltration of inflammatory cells into lesion the areas (Voskuhl et al. 2009). In addition, there are also reports supported astrocyte protective role in formation of new myelin sheath in demyelinated areas through mediating microglia recruitment to the injured sites for removing debris formed in these regions, a prerequisite factor for retaining oligodendrocyte generation (Skripuletz et al. 2012).

In contrasting to the studies mentioned above, there is compelling evidence for astrocytes acting in a complete diverse way by secreting inflammatory chemokines such as CXCL10 and CXCL12 to the lesion areas for promoting recruitment of inflammatory cells such as microglia toward these sites (Bianchi et al. 2011; Qin and Benveniste 2012). In addition, recent studies attested that the astrocytic scars formed at the lesion areas act as physical and biochemical barriers for remyelination processes. These scars is believed to create an unfavorable and inhibitory extracellular microenvironment for inhibiting survival, migration and differentiation of OPCs in the chronic MS lesions (Li et al. 2011; Yamamoto et al. 2014).

We examined the rate expressions for astrocytic chemokines *CXCL10* and *CXCL12* that are responsible for recruitment of microglia. We noticed a fall in the rate of expressions for the two chemokines in the astrocyte-ablated animals. Downregulation of *CXCL10* after astrocyte ablation is also approved in the study carried out by Skripuletz et al. (2012). Microglia expresses CXCR3 that is a putative receptor for CXCL10. Interaction between CXCR3 with CXCL10 is contributed to the migration of microglia toward the site of injury (Biber et al. 2002; Rappert et al. 2004; Skripuletz et al. 2012). Tanuma et al. in MS patients showed a high rate of expression for CXCL10 in astrocytes at the rim of demyelinating

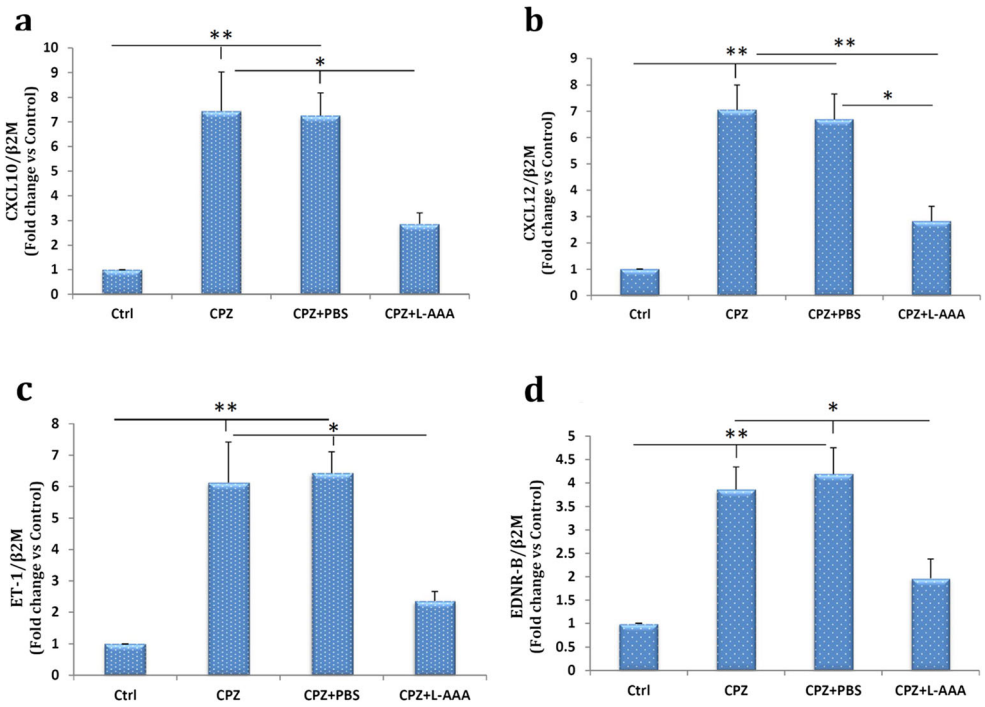

Fig. 7 Effect of astrocyte ablation on mRNA expression of chemokines CXCL10 and CXCL12, and signaling peptides ET-1 and EDNRB in the corpus callosum. Animals receiving cuprizone showed a considerable increase in the rate of expressions for all of the chemokines (for all $p < 0.01$ vs. control), which were counteracted after administration of L-AAA. ($n = 3$ per group) * $p < 0.05$, ** $p < 0.01$, and *** $p < 0.001$ (ANOVA followed by post-hoc analysis)

plaques (Tanuma et al. 2006). Astroglial CXCL10 deletion is reported to be involved in reduction of clinical deficits and acute demyelination in EAE mice (Ransohoff et al. 1993; Ko et al. 2014).

It is important to note that OPCs have the capacity to differentiate into myelin-producing oligodendrocytes in demyelinating areas, but this differentiation is often unsuccessful in chronic demyelinating injuries due to release of inhibitory factors from reactive astrocytes in these pathological conditions (McKhann 1982; Chang et al. 2002; Hammond et al. 2014). LINGO-1 is a CNS-specific transmembrane signaling protein known as a potent negative regulator against differentiation of OPCs into matured oligodendrocytes, and thereby restricting retaining of axonal myelination (Foale et al. 2017). In addition, reactive astrocytes secrete factors like ET-1 (Gadea et al. 2009) and EDNR (Hammond et al. 2015) to restrict OPC differentiation. ET-1 also has astrogliosis effects attested both in vitro and in vivo (D'haeseleer et al. 2013; Hammond et al. 2014). We found an increase in the rate expressions for both *ET-1* and *EDNR* in the mice exposed to the cuprizone. These changes were counteracted after administration of L-AAA. ET-1 activity on suppression of OPC differentiation is exerts through two possible mechanisms: direct and indirect signaling. In the direct signaling, ET-1 through activation of EDNRs expressed on surface of OPCs suppresses their differentiation in particular during the migration of the cells. In an indirect mechanism, ET-1 induces release of Jagged1 from astrocytes. Jagged1 is a ligand for Notch1 receptor expressed on surface of OPCs (John et al. 2002; Gadea et al. 2009). Interaction between Jagged1 with Notch1 could inhibit OPC differentiation and further remyelination-associated processes (Zhang et al. 2009; Hammond et al. 2014).

Conclusion

From data of the current study we conclude that ablation of astrocytes in the demyelinated MS injury could improve remyelination. This improvement was related to a rise in the number and maturation of $Olig2^+$ cells in the lesion areas possibly through hampering microgliosis and astrogliosis related mechanisms. Results of this study suggest that astrocyte ablation could be exploited as a promising therapeutic targeting for promotion of myelin recovery in demyelinated tissue despite having controversial claims either in favor or against application of this strategy.

Acknowledgments The present study has been supported by Tehran University of Medical Sciences and Health Services, Tehran, Iran (Grant number 95-04-30-33652).

Compliance with ethical standards

Conflict of interest The authors declare no conflicts of interest.

References

Acs P, Kipp M, Norkute A, Johann S, Clarner T, Braun A, Berente Z, Komoly S, Beyer C (2009) 17β-estradiol and progesterone prevent cuprizone provoked demyelination of corpus callosum in male mice. Glia 57(8):807–814

Aryanpour R, Pasbakhsh P, Zibara K, Namjoo Z, Boroujeni FB, Shahbeigi S, Kashani IR, Beyer C, Zendehdel A (2017) Progesterone therapy induces an M1 to M2 switch in microglia phenotype and suppresses NLRP3 inflammasome in a cuprizone-induced demyelination mouse model. Int Immunopharmacol 51: 131–139

Back SA, Tuohy TM, Chen H, Wallingford N, Craig A, Struve J, Luo NL, Banine F, Liu Y, Chang A (2005) Hyaluronan accumulates in demyelinated lesions and inhibits oligodendrocyte progenitor maturation. Nat Med 11(9):966–972

Baron W, Colognato H, Ffrench-Constant C (2005) Integrin-growth factor interactions as regulators of oligodendroglial development and function. Glia 49(4):467–479

Bianchi R, Kastrisianaki E, Giambanco I, Donato R (2011) S100B protein stimulates microglia migration via RAGE-dependent up-regulation of chemokine expression and release. J Biol Chem 286(9): 7214–7226

Biber K, Dijkstra I, Trebst C, De Groot C, Ransohoff R, Boddeke H (2002) Functional expression of CXCR3 in cultured mouse and human astrocytes and microglia. Neuroscience 112(3):487–497

Chang A, Tourtellotte WW, Rudick R, Trapp BD (2002) Premyelinating oligodendrocytes in chronic lesions of multiple sclerosis. N Engl J Med 346(3):165–173

Chari D, Huang W, Blakemore W (2003) Dysfunctional oligodendrocyte progenitor cell (OPC) populations may inhibit repopulation of OPC depleted tissue. J Neurosci Res 73(6):787–793

Clemente D, Ortega MC, Melero-Jerez C, De Castro F (2013) The effect of glia-glia interactions on oligodendrocyte precursor cell biology during development and in demyelinating diseases. Front Cell Neurosci 7:268

Correale J, Farez MF (2015) The role of astrocytes in multiple sclerosis progression. Front Neurol 6:180

D'haeseleer M, Beelen R, Fierens Y, Cambron M, Vanbinst A-M, Verborgh C, Demey J, De Keyser J (2013) Cerebral hypoperfusion in multiple sclerosis is reversible and mediated by endothelin-1. Proc Natl Acad Sci USA 110(14):5654–5658

Foale S, Berry M, Logan A, Fulton D, Ahmed Z (2017) LINGO-1 and AMIGO3, potential therapeutic targets for neurological and dysmyelinating disorders? Neural Regen Res 12(8):1247

Franklin RJ, Kotter MR (2008) The biology of CNS remyelination. J Neurol 255(1):19–25

Frohman EM, Racke MK, Raine CS (2006) Multiple sclerosis—the plaque and its pathogenesis. N Engl J Med 354(9):942–955

Gadea A, Aguirre A, Haydar TF, Gallo V (2009) Endothelin-1 regulates oligodendrocyte development. J Neurosci 29(32):10047–10062

Ghareghani M, Ghanbari A, Dokoohaki S, Farhadi N, Hosseini SM, Mohammadi R, Sadeghi H (2016) Methylprednisolone improves lactate metabolism through reduction of elevated serum lactate in rat model of multiple sclerosis. Biomed Pharmacother 84:1504–1509

Gochenauer GE, Robinson MB (2001) Dibutyryl-cAMP (dbcAMP) up-regulates astrocytic chloride-dependent l-[3H] glutamate transport and expression of both system xc− subunits. J Neurochem 78(2): 276–286

Hammond TR, Gadea A, Dupree J, Kerninon C, Nait-Oumesmar B, Aguirre A, Gallo V (2014) Astrocyte-derived endothelin-1 inhibits remyelination through notch activation. Neuron 81(3):588–602

Hammond TR, McEllin B, Morton PD, Raymond M, Dupree J, Gallo V (2015) Endothelin-B receptor activation in astrocytes regulates the rate of oligodendrocyte regeneration during remyelination. Cell Rep 13(10):2090–2097

John GR, Shankar SL, Shafit-Zagardo B, Massimi A, Lee SC, Raine CS, Brosnan CF (2002) Multiple sclerosis: re-expression of a developmental pathway that restricts oligodendrocyte maturation. Nat Med 8(10):1115–1121

Karussis D, Karageorgiou C, Vaknin-Dembinsky A, Gowda-Kurkalli B, Gomori JM, Kassis I, Bulte JW, Petrou P, Ben-Hur T, Abramsky O (2010) Safety and immunological effects of mesenchymal stem cell transplantation in patients with multiple sclerosis and amyotrophic lateral sclerosis. Arch Neurol 67(10):1187–1194

Khurgel M, Koo AC, Ivy GO (1996) Selective ablation of astrocytes by intracerebral injections of α-aminoadipate. Glia 16(4):351–358

Kieseier BC, Stüve O (2011) A critical appraisal of treatment decisions in multiple sclerosis—old versus new. Nat Rev Neurol 7(5):255–262

Kipp M, Clarner T, Dang J, Copray S, Beyer C (2009) The cuprizone animal model: new insights into an old story. Acta Neuropathol 118(6):723–736

Ko EM, Ma JH, Guo F, Miers L, Lee E, Bannerman P, Burns T, Ko D, Sohn J, Soulika AM (2014) Deletion of astroglial CXCL10 delays clinical onset but does not affect progressive axon loss in a murine autoimmune multiple sclerosis model. J Neuroinflammation 11(1): 105

Li Z-W, Tang R-H, Zhang J-P, Tang Z-P, Qu W-S, Zhu W-H, Li J-J, Xie M-J, Tian D-S, Wang W (2011) Inhibiting epidermal growth factor receptor attenuates reactive astrogliosis and improves functional outcome after spinal cord injury in rats. Neurochem Int 58(7):812–819

McKhann GM (1982) Guillain-Barré syndrome is there a role for plasmapheresis? An update. Neurology 32(11):1282–1282

Nair A, Frederick TJ, Miller SD (2008) Astrocytes in multiple sclerosis: a product of their environment. Cell Mol Life Sci 65(17):2702–2720

Nessler J, Bénardais K, Gudi V, Hoffmann A, Tejedor LS, Janßen S, Prajeeth CK, Baumgärtner W, Kavelaars A, Heijnen CJ (2013) Effects of murine and human bone marrow-derived mesenchymal stem cells on cuprizone induced demyelination. PLoS One 8(7): e69795

Nishimura R, Santos D, Fu S-T, Dwyer B (2000) Induction of cell death by L-alpha-aminoadipic acid exposure in cultured rat astrocytes: relationship to protein synthesis. Neurotoxicology 21(3):313–320

Qin H, Benveniste EN (2012) ELISA methodology to quantify astrocyte production of cytokines/chemokines in vitro. Methods Mol Biol 814:235–249

Ransohoff RM, Hamilton TA, Tani M, Stoler MH, Shick HE, Major JA, Estes ML, Thomas DM, Tuohy VK (1993) Astrocyte expression of mRNA encoding cytokines IP-10 and JE/MCP-1 in experimental autoimmune encephalomyelitis. FASEB J 7(6):592–600

Rappert A, Bechmann I, Pivneva T, Mahlo J, Biber K, Nolte C, Kovac AD, Gerard C, Boddeke HW, Nitsch R (2004) CXCR3-dependent microglial recruitment is essential for dendrite loss after brain lesion. J Neurosci 24(39):8500–8509

Skripuletz T, Gudi V, Hackstette D, Stangel M (2011) De-and remyelination in the CNS white and grey matter induced by cuprizone: the old, the new, and the unexpected. Histol Histopathol 26(12):1585–1597

Skripuletz T, Hackstette D, Bauer K, Gudi V, Pul R, Voss E, Berger K, Kipp M, Baumgärtner W, Stangel M (2012) Astrocytes regulate myelin clearance through recruitment of microglia during cuprizone-induced demyelination. Brain 136(1):147–167

Stoffels JM, de Jonge JC, Stancic M, Nomden A, van Strien ME, Ma D, Šišková Z, Maier O, Ffrench-Constant C, Franklin RJ (2013) Fibronectin aggregation in multiple sclerosis lesions impairs remyelination. Brain 136(1):116–131

Stoffels JM, Hoekstra D, Franklin RJ, Baron W, Zhao C (2015) The EIIIA domain from astrocyte-derived fibronectin mediates proliferation of

oligodendrocyte progenitor cells following CNS demyelination. Glia 63(2):242–256

Tanuma N, Sakuma H, Sasaki A, Matsumoto Y (2006) Chemokine expression by astrocytes plays a role in microglia/macrophage activation and subsequent neurodegeneration in secondary progressive multiple sclerosis. Acta Neuropathol 112(2):195–204

Tsai MJ, Chang Y-F, Schwarcz R, Brookes N (1996) Characterization ofl-α-aminoadipic acid transport in cultured rat astrocytes. Brain Res 741(1–2):166–173

Voskuhl RR, Peterson RS, Song B, Ao Y, Morales LBJ, Tiwari-Woodruff S, Sofroniew MV (2009) Reactive astrocytes form scar-like perivascular barriers to leukocytes during adaptive immune inflammation of the CNS. J Neurosci 29(37):11511–11522

Williams A, Piaton G, Aigrot M-S, Belhadi A, Théaudin M, Petermann F, Thomas J-L, Zalc B, Lubetzki C (2007a) Semaphorin 3A and 3F: key players in myelin repair in multiple sclerosis? Brain 130(10): 2554–2565

Williams A, Piaton G, Lubetzki C (2007b) Astrocytes—friends or foes in multiple sclerosis? Glia 55(13):1300–1312

Yamamoto S, Gotoh M, Kawamura Y, Yamashina K, Yagishita S, Awaji T, Tanaka M, Maruyama K, Murakami-Murofushi K, Yoshikawa K (2014) Cyclic phosphatidic acid treatment suppress cuprizone-induced demyelination and motor dysfunction in mice. Eur J Pharmacol 741:17–24

Zhang Y, Argaw AT, Gurfein BT, Zameer A, Snyder BJ, Ge C, Lu QR, Rowitch DH, Raine CS, Brosnan CF (2009) Notch1 signaling plays a role in regulating precursor differentiation during CNS remyelination. Proc Natl Acad Sci USA 106(45):19162–19167